ANALYTIC MODEL OF THE CYLINDRICAL SHELL MOTION EQUATIONS

Mario Francisco Guerra Boaratti
Instituto de Pesquisas Energéticas e Nucleares (IPEN / CNEN - SP)
Av. Professor Lineu Prestes 2242
05508-000 São Paulo, SP
boaratti@usp.br

Daniel Kao Sun Ting
Instituto de Pesquisas Energéticas e Nucleares (IPEN / CNEN - SP)
Av. Professor Lineu Prestes 2242
05508-000 São Paulo, SP
dksting@ipen.br

Abstract. *Leaks in pressurized tubes generate acoustic waves that propagate through the walls of these tubes, which can be captured by accelerometers or by acoustic emission sensors. The knowledge of how these walls can vibrate, or in another way, how these acoustic waves propagate in this material is fundamental in the detection and localization process of the leak source. The objective of this paper is to present an analytic model, through the derivation and solution of the motion equations of a cylindrical shell, which allows visualizing the behavior of the tube surface excited by a point source. Since the cylindrical surface has a closed pattern in the circumferential direction, waves that are beginning their trajectory will meet with another that has already completed the turn over the cylindrical shell, in the clockwise direction as well as in the counter clockwise direction, generating constructive and destructive interferences. After enough time of propagation, peaks and valleys in the shell surface are formed, which can be visualized through a graphic representation of the analytic solution. To check the theoretical results, measures were performed in an experimental setup, with the objective of mapping the tube surface accelerations and displacements when a point source is excited at several frequencies. The comparisons showed an excellent agreement between the theoretical results and the experimental mapping, validating thus the analytic model.*

Keywords: *shell, leak, model*

1. Introduction

The integrity of pressurized tubes in nuclear and industrial processes is fundamental, where leaks can lead to the situations of risks, financial losses and severe environmental impacts. Particularly, in the primary loops of a nuclear power plant, the use of a validated leak detection system is a design requirement for the licensing and operation under the leak before break criteria. The theoretical and experimental studies presented in this paper are part of the development of a novel leak detection system for the primary piping of a nuclear plant.

Leaks in pressurized tubes generate stress waves that propagate through the walls of these tubes, which can be captured by accelerometers or by acoustic emission sensors.

The knowledge of how these walls can vibrate, or in another way, how these stress waves propagate in this material is fundamental in the development of a detection and localization method of the leak source. The objective of this paper is to develop an analytic model, through the derivation and solution of the motion equations for a cylindrical shell, which allows for the simulation of the behavior of the tube surface excited by a point source.

When a solid body is excited by an impact or by an abrupt displacement, it generates a dynamic problem, which is modeled by the corresponding movement equations. When a solid is loaded dynamically, it is observed that its response is not transmitted instantly to every position. Stress and deformation waves will appear and they will be irradiated in all directions inside this solid with finite velocities. A point located at a certain distance from the source position will only feel its effect after some time. For the present work, we considered the tube as being an infinite cylindrical shell, composed of an elastic, homogeneous and isotropic material, with an average radius a and a constant wall thickness h, being the thickness small compared to the radius. It was also considered that the displacements are small compared with the thickness, and that the only external load acts at the cylindrical shell surface. The external load is a harmonic point source, which generates waves with crests that move away radially from the excitation point. The derived equations of motion are shown in Eq. (1), below.

These equations describe the harmonic vibration of a thin cylindrical shell according to the Flügge theory of thin shells. They are used here in the simplified form according to the Donnell formulation, presented in Blevins (1995), Junger (1986), Fuller (1982, 1983, 1986), Xu *et al.* (1998, 1999, 2000) and Amabili (1996). They solved Eq. (1) subjected to a harmonic localized belt like source function.

$$\frac{\partial^2 u}{\partial x^2}+\frac{1-\nu}{2a^2}\frac{\partial^2 u}{\partial \theta^2}+\frac{1+\nu}{2a}\frac{\partial^2 v}{\partial x \partial \theta}+\frac{\nu}{a}\frac{\partial w}{\partial x}-\frac{1}{c_p{}^2}\frac{\partial^2 u}{\partial t^2}=0$$

$$\frac{(1+\nu)}{2a}\frac{\partial^2 u}{\partial x \partial \theta}+\frac{(1-\nu)}{2}\frac{\partial^2 v}{\partial x^2}+\frac{1}{a^2}\frac{\partial^2 v}{\partial \theta^2}+\frac{1}{a^2}\frac{\partial w}{\partial \theta}-\frac{1}{c_p{}^2}\frac{\partial^2 v}{\partial t^2}=0$$

$$\frac{\nu}{a}\frac{\partial u}{\partial x}+\frac{1}{a^2}\frac{\partial v}{\partial \theta}+\frac{w}{a^2}+\beta^2\left(a^2\frac{\partial^4 w}{\partial x^4}+2\frac{\partial^4 w}{\partial x^2 \partial \theta^2}+\frac{1}{a^2}\frac{\partial^4 w}{\partial \theta^4}\right)+\frac{1}{c_p{}^2}\frac{\partial^2 w}{\partial t^2}-\frac{p_a(1-\nu^2)}{Eh}=0 \quad (1)$$

In this present work, a point source will be considered, which introduced significant difficulties since two Dirac functions are needed to represent such a source. The solution for the transient analytic model, which is bi-dimensional in the axial and circumferential directions, was derived using the two-dimensional Fourier Transform and the Residues method for obtaining the eigenvalues.

Since the cylindrical surface has a closed pattern in the circumferential direction, waves that are beginning their trajectory will meet with another that has already completed the turn over the cylindrical shell, in the clockwise direction as well as in the counter clockwise direction, generating constructive and destructive interferences. After enough time of propagation, peaks and valleys in the shell surface are formed, which can be visualized through a graphic representation of the analytic solution.

It can be seen that surface waves with helical paths wrap up over the cylindrical surface, so that the wave that leaves with a smaller angle in relation to the axial direction, arrives to a certain point in the surface of the cylinder before the wave that leaves with larger angle and it needs to complete several loops around of the cylinder before reaching the same point. This phenomenon generates phase delay between the waves that propagate on different paths around the cylinder before they meet again. If the excitation source has a defined frequency, after an enough time, a stationary state is reached, creating points of displacements peaks and valley on the shell surface.

To check the theoretical results, experimental measurements were performed in an experimental setup, with the objective of mapping the tube surface accelerations where a point source is excited with several different frequencies. The comparisons showed an excellent agreement between the theoretical results and the experimental mapping, validating thus the analytic model.

2. Analytic solution for the mathematical model

As already mentioned, we considered the tube as an infinite cylindrical shell, constituted by an elastic, homogeneous and isotropic material, surrounded by vacuum. The cylindrical coordinates system (x, θ, r), describe by Figure 1 was used, where x is the axial shell direction, θ is the angle in the circumferential direction, r is the radial direction, a is the average radius of the shell and h is the wall thickness, being the thickness small compared to the radius and constant along the tube. The values u, v and w represent the components of displacement at the shell surface in the axial, circumferential and radial directions, respectively.

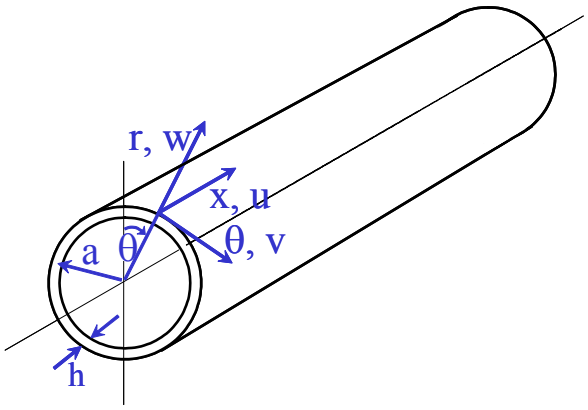

Figure 1. Cylindrical shell coordinate system.

The components of the wave displacement that propagate in a thin cylindrical shell can be expressed in the form of a harmonic series, as shown in the Eq. (2), Eq. (3) and Eq. (4), according to Fuller (1982, 1983), Xu *et al.* (1998, 1999), Feng (1994) and Ming *et al.* (2000).

$$u = \sum_{s=0}^{\infty}\sum_{n=0}^{\infty} U_{ns}\cos(n\theta)e^{ik_{ns}x}e^{i\omega t}e^{i\pi/2} \tag{2}$$

$$v = \sum_{s=0}^{\infty}\sum_{n=0}^{\infty} V_{ns}\sin(n\theta)e^{ik_{ns}x}e^{i\omega t}e^{-i\pi/2} \tag{3}$$

$$w = \sum_{s=0}^{\infty}\sum_{n=0}^{\infty} W_{ns}\cos(n\theta)e^{ik_{ns}x}e^{i\omega t} \tag{4}$$

In the equations above, ω is the frequency in radian, n is the circumferential modal number, which can be seen in Figure 2, k_{ns} is the axial wave number and subscript s corresponds to the solutions of the axial wave numbers.

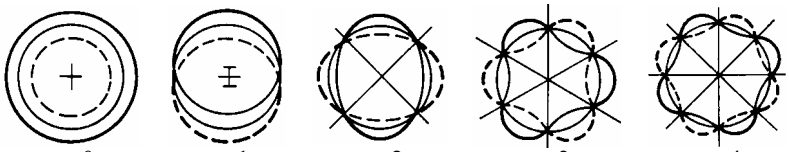

Figure 2. Circumferential modal patterns for the cylindrical shell.

The point source will be considered as a harmonic forcing function with amplitude F0 applied in the positions x = 0 and θ = 0, of the type:

$$P_a(t) = F_0\,\delta(\theta)\delta(x)e^{i\omega t} \tag{5}$$

Due to the presence of the Dirac function in x = 0 and θ = 0, it is convenient to express the displacements and the applied force as Double Fourier Transforms as shown below.

$$u = \left(\frac{1}{\sqrt{2\pi}}\right)^2 \int_{-\infty}^{\infty}\int_{-\infty}^{\infty}\sum_{n=0}^{\infty}\sum_{s=0}^{\infty}\overline{\overline{U_{ns}}}\,e^{i\omega t}e^{i\pi/2}\,e^{ik_{ns}x}\,e^{in\theta}dk_{ns}\,dn \tag{6}$$

$$v = \left(\frac{1}{\sqrt{2\pi}}\right)^2 \int_{-\infty}^{\infty}\int_{-\infty}^{\infty}\sum_{n=0}^{\infty}\sum_{s=0}^{\infty}\overline{\overline{V_{ns}}}\,e^{i\omega t}e^{-i\pi/2}\,e^{ik_{ns}x}\,e^{in\theta}dk_{ns}\,dn \tag{7}$$

$$w = \left(\frac{1}{\sqrt{2\pi}}\right)^2 \int_{-\infty}^{\infty}\int_{-\infty}^{\infty}\sum_{n=0}^{\infty}\sum_{s=0}^{\infty}\overline{\overline{W_{ns}}}\,e^{i\omega t}\,e^{ik_{ns}x}\,e^{in\theta}dk_{ns}\,dn \tag{8}$$

$$p_a = \left(\frac{1}{\sqrt{2\pi}}\right)^2 \int_{-\infty}^{\infty}\int_{-\infty}^{\infty}\sum_{n=0}^{\infty}\sum_{s=0}^{\infty}\frac{F_0\,e^{i\omega t}}{2\pi}e^{ik_{ns}x}\,e^{in\theta}dk_{ns}\,dn \tag{9}$$

Here, the terms $\overline{\overline{U_{ns}}}$, $\overline{\overline{V_{ns}}}$ e $\overline{\overline{W_{ns}}}$ are the double Fourier transforms of the Eq. (2), Eq. (3) and Eq. (4). Developing the partial derivatives of the Eq. (6), Eq. (7) and Eq. (8), and substituting these derivatives in the equation of the movement, Eq. (1), the solution in matrix form is obtained:

$$\begin{bmatrix} \Omega^2 - \frac{n^2(1-\nu)}{2} - k_{ns}^2 a^2 + & \frac{n(1+\nu)}{2} k_{ns} a & \nu k_{ns} a \\ -\frac{n(1+\nu)}{2} k_{ns} a & -\Omega^2 + n^2 + \frac{1-\nu}{2} k_{ns}^2 a^2 & n \\ -\nu k_{ns} a & n & 1+\beta^2\left(k_{ns}^2 a^2 + n^2\right)^2 - \Omega^2 \end{bmatrix} \cdot \begin{bmatrix} \overline{\overline{U_{ns}}} \\ \overline{\overline{V_{ns}}} \\ \overline{\overline{W_{ns}}} \end{bmatrix} = \begin{bmatrix} 0 \\ 0 \\ \frac{F_0(1-\nu^2)a^2}{2\pi E h} \end{bmatrix} \tag{10}$$

Where the normalized frequency Ω is defined by $\Omega = \frac{\omega a}{c_p}$, Fuller (1982, 1983, 1986), Junger (1986), Feng (1994) and Xu *et al.* (1998, 1999, 2000), in the which the velocity c_p is given by the equation $c_p = \sqrt{\frac{E}{(1-\nu^2)\rho}}$, E is the elasticity module, ρ is the material density and ν is the Poisson coefficient.

Naming $\left|\mathrm{I}\right|$ as the inverse of the coefficient matrix of Eq. (10) and solving for $\overline{\overline{U_{ns}}}$, $\overline{\overline{V_{ns}}}$ e $\overline{\overline{W_{ns}}}$, one has:

$$\begin{bmatrix} \overline{\overline{U_{ns}}} \\ \overline{\overline{V_{ns}}} \\ \overline{\overline{W_{ns}}} \end{bmatrix} = \frac{F_0(1-\nu^2)a^2}{2\pi E h} \begin{bmatrix} \mathrm{I}_{13} \\ \mathrm{I}_{23} \\ \mathrm{I}_{33} \end{bmatrix} \tag{11}$$

Substituting $\overline{\overline{U_{ns}}}$, $\overline{\overline{V_{ns}}}$ e $\overline{\overline{W_{ns}}}$ from the Eq. (11) in the Eq. (6), Eq. (7) and Eq. (8) and applying the double inverse Fourier Transforms, the displacements are obtained in the three directions:

$$\begin{bmatrix} u \\ v \\ w \end{bmatrix} = \frac{F_0(1-\nu^2)a^2}{2\pi E h} e^{i\omega t} \sum_{n=0}^{\infty}\sum_{s=0}^{\infty} \begin{bmatrix} \left(\frac{1}{\sqrt{2\pi}}\right)^2 \int_{-\infty}^{\infty}\int_{-\infty}^{\infty} (\mathrm{I}_{13})_{ns}\, e^{i\pi/2}\, e^{ik_{ns}x}\, dk_{ns}\, e^{in\theta}\, dn \\ \left(\frac{1}{\sqrt{2\pi}}\right)^2 \int_{-\infty}^{\infty}\int_{-\infty}^{\infty} (\mathrm{I}_{23})_{ns}\, e^{-i\pi/2}\, e^{ik_{ns}x}\, dk_{ns}\, e^{in\theta}\, dn \\ \left(\frac{1}{\sqrt{2\pi}}\right)^2 \int_{-\infty}^{\infty}\int_{-\infty}^{\infty} (\mathrm{I}_{33})_{ns}\, e^{ik_{ns}x}\, dk_{ns}\, e^{in\theta}\, dn \end{bmatrix} \tag{12}$$

Considering that the solution of the integral in n only exists for n = 0, 1, 2, 3…∞, this integral becomes a cumulative sum in n. The other integral can be solved through the residues theorem.

$$\begin{bmatrix} u \\ v \\ w \end{bmatrix} = \frac{F_0(1-\nu^2)a^2}{2\pi E h} e^{i\omega t} \begin{bmatrix} \frac{1}{2\pi}\sum_{n=0}^{\infty} 2\pi i \left(\sum_{s=0}^{\infty}\left(\mathrm{Res}((\mathrm{I}_{13})_{ns}\, e^{ik_{ns}x}\right)\right) e^{i\pi/2} e^{in\theta} \\ \frac{1}{2\pi}\sum_{n=0}^{\infty} 2\pi i \left(\sum_{s=0}^{\infty}\left(\mathrm{Res}((\mathrm{I}_{23})_{ns}\, e^{ik_{ns}x}\right)\right) e^{-i\pi/2} e^{in\theta} \\ \frac{1}{2\pi}\sum_{n=0}^{\infty} 2\pi i \left(\sum_{s=0}^{\infty}\left(\mathrm{Res}((\mathrm{I}_{33})_{ns}\, e^{ik_{ns}x}\right)\right) e^{in\theta} \end{bmatrix} \tag{13}$$

The Eq. (13) is solved using numerical computational technique, based on Matlab[1] to obtain the numeric solution for u, v and w for all the *n* and *s* as function of x, θ and t.

3. Mathematical Model Validation

3.1. The experimental setup

The experimental setup used to validate the mathematical model, is composed by a carbon steel tube, 6 m long, 10 cm average radius, 4,7 mm wall average thickness. With the objective of simulating an infinite tube condition the

[1] Trade mark of the The Math Works, Inc.

tube end sides were introduced in dry sand boxes, technique also used by Feng (1996) and Ming *et al.* (2000). In this case, the sand works as a trap for the waves that arrive, avoiding that these find the way back for the wall tube. In this assembly the tube was introduced 30 cm inside of the sand.

3.2. Tube mapping

With the objective of verifying the behavior of the waves propagations on the cylindrical shell surface, the tube surface was mapped. The measurements were accomplished using accelerometers distributed properly and fixed on its surface. To simulate the point excitation source, a small piezoelectric disc was used connected to a sine function generator where both frequency and output voltage are adjustable. At the excitation source, an accelerometer was also installed, which has the purpose of synchronizing all the measurements from the other accelerometers. The experiments were carried out for several different frequencies. Here, for brevity we will only present the results for 2 KHz point source.

Figure 3 shows the result of this mapping along an axial line with accelerometers spaced 5 cm apart. Here, in the illustration, the red represents the peaks and the blue the valleys.

Applying the same conditions in the Eq. (13), it is obtained the cylindrical shell theoretical response shown in Figure 4. It is observed in a first qualitative analysis, a likeness in the patterns with relationship to the positions of the maximum and minimum points along the wave propagation. This agreement between measured and simulated mapping is maintained for other source frequencies.

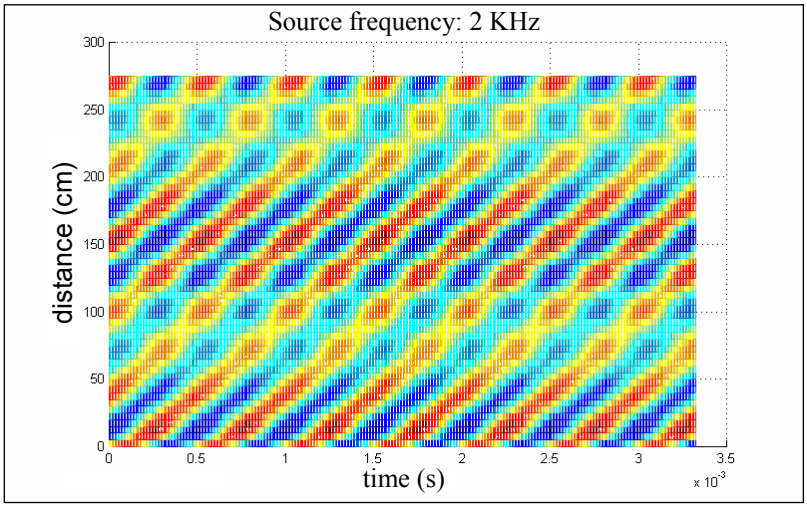

Figure 3. 3D view of the measured radial displacement (w) for θ = 0°.

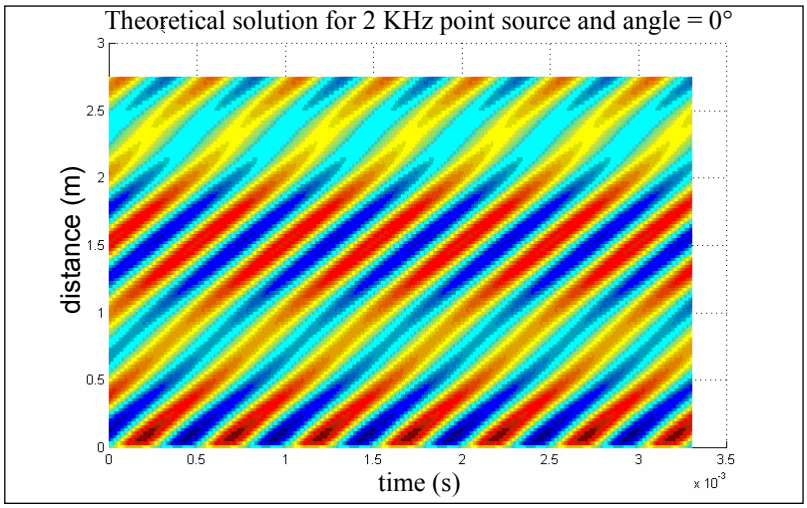

Figure 4. 3D view of the calculated radial displacement (w) for θ = 0°.

To have a more quantitative comparison, the time behavior in some positions on the tube was chosen. This is like taking slices at given positions from Figure 3 and Figure 4. The Figure 5 shows the time function at the following the surface positions: source (sensor A), 20 cm (sensor B), 40 cm (sensor C) and 60 cm (sensor D) from source.

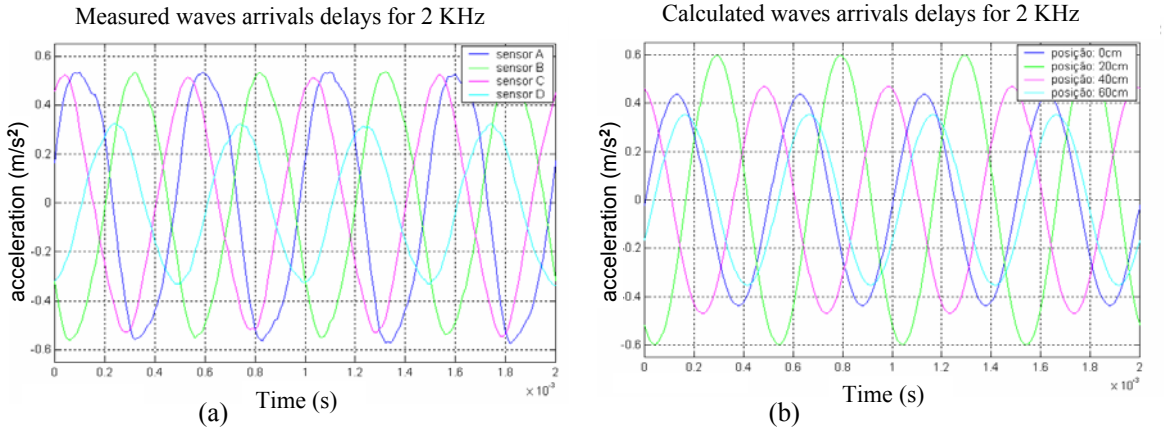

Figure 5. Comparison in time plot between (a) measured and (b) theoretical propagation waves for a 2 KHz source.

These propagations time delays are related to the effective stationary waves velocities. In subsequent Tab. 1 and Tab. 2, the effective delays and the respective velocities for the chosen measurement positions and the corresponding calculated values using the theoretical model, in three frequencies, are presented. To obtain the time delays, the waves cross-correlation was used, taking as reference the source position as the origin. The velocity is calculated by the relationship $\Lambda = v/f$, where Λ is the wave length and f is the source frequency. One should observe here, that the stationary wave velocity is smaller than the extensional wave propagation speed in the steel, c_p, that is approximately 5200 m/s, and than the traverse wave velocity in the solid that is approximately 3100 m/s in the steel.

Table 1. Time delays and theoretical velocities

	1 KHz		2 KHz		3 KHz	
distance	Δt (s)	velocity (m/s)	Δt (s)	velocity (m/s)	Δt (s)	velocity (m/s)
0,2 m	1,55E-04	1290,32	1,66E-04	1204,82	1,65E-04	1212,12
0,4 m	3,10E-04	1290,32	3,63E-04	1101,93	2,80E-04	1428,57
0,6 m	5,50E-04	1090,91	5,62E-04	1067,62	4,00E-04	1500,00
velocities average:		**1223,85**		**1124,79**		**1380,23**

Table 2. Time delays and measured velocities

	1 KHz		2 KHz		3 KHz	
distance	Δt (s)	velocity (m/s)	Δt (s)	velocity (m/s)	Δt (s)	velocity (m/s)
0,2 m	2,30E-04	869,57	2,10E-04	952,38	2,00E-04	1000,00
0,4 m	3,30E-04	1212,12	3,70E-04	1081,08	2,50E-04	1600,00
0,6 m	6,00E-04	1000,00	6,10E-04	983,61	4,00E-04	1500,00
velocities average:		**1027,23**		**1005,69**		**1366,67**

4. Conclusions

It can be observed that the theoretical model represents with good precision the behavior of a cylindrical shell so much in the time as well as in distance for the axial and circumferential directions. The model is also capable to show the behavior of the shell in the spatial domain for a given instant or its response in frequency. Such situations were compared with those measured in the real shell and the comparisons presented excellent results.

5. References

Amabili, M., 1996, "Free Vibration of Partially Filled, Horizontal Cylindrical Shells," Journal of Sound and Vibration, vol. 191, No. 5, pp.757-780.

Blevins, R. D., 1995, "Formulas for Natural Frequency and Mode Shape", Krieger Publishing Company, USA.

Feng, L., 1994, "Acoustic Properties of Fluid-Filled Elastic Pipes," Journal of Sound and Vibration, vol. 176, No. 3, pp.399-413.

Feng, L., 1996, "Experimental Studies of the Acoustic Properties of a Finite Elastic Pipe Filled with Water/Air," Journal of Sound and Vibration, vol. 189, No. 4, pp.511-524.

Fuller, C. R., Fahy, F. J., 1982, "Characteristics of Wave Propagation and Energy Distributions in Cylindrical Elastic Shells Filled with Fluid", Journal of Sound and Vibration, vol. 81, No. 4, pp.501-518.

Fuller, C. R., 1983, "The Input Mobility of an Infinite Circular Cylindrical Elastic Shell Filled with Fluid," Journal of Sound and Vibration, vol. 87, No. 3, pp.409-427.

Fuller, C. R., 1986, "Radiation of Sound from an Infinite Cylindrical Elastic Shell Excited by an Internal Monopole Source," Journal of Sound and Vibration, vol. 109, No. 2, pp.259-275.

Junger, M. C., Feit, D., 1986, "Sound, Structures, and Their Interaction", The MIT Press, USA, 2.ed.

Ming, R., Pan, J., Norton, M. P., 2000, "The Measurement of Structural Mobilities of a Circular Cylindrical Shell," Journal of Acoustic Society of America, vol. 107, No. 3, Mar..

Xu, M. B., Zhang, X. M., 1998, "Vibrational Power Flow in a Fluid-Filled Cylindrical Shell," Journal of Sound and Vibration, vol. 218, No. 4, pp.587-598.

Xu, M. B., Zhang, W. H., 1999, "The Effect of Wall Joint on the Vibrational Power Flow Propagation in a Fluid-Filled Shell," Journal of Sound and Vibration, vol. 224, No. 3, pp.395-410.

Xu M. B., Zhang W. H., 2000, "Vibrational Power Flow Input and Transmission in a Circular Cylindrical Shell Filled with Fluid," Journal of Sound and Vibration, vol. 234, No. 3, pp.387-403.

6. Responsibility notice

The author(s) is (are) the only responsible for the printed material included in this paper.